Electronic Supplementary Material (ESI) for Journal of Materials Chemistry A.

High entropy spinel oxide nanoparticles for superior lithiation-delithiation performance

Nguyen Thi Xuyen [1], Jagabandhu Patra [2,3], Jeng-Kuei Chang [2*], Jyh-Ming Ting [1*]

[1] Department of Materials Science and Engineering, National Cheng Kung University

1 University Road, Tainan 70101, Taiwan

[2] Department of Materials Science and Engineering, National Chiao Tung University

1001 University Road, Hsinchu 30010, Taiwan

[3] Hierarchical Green-Energy Materials (Hi-GEM) Research Center, National Cheng Kung University, Tainan 70101, Taiwan

* Corresponding authors:

Jeng-Kuei Chang (jkchang@nctu.edu.tw)

Jyh-Ming Ting (jting@mail.ncku.edu.tw)

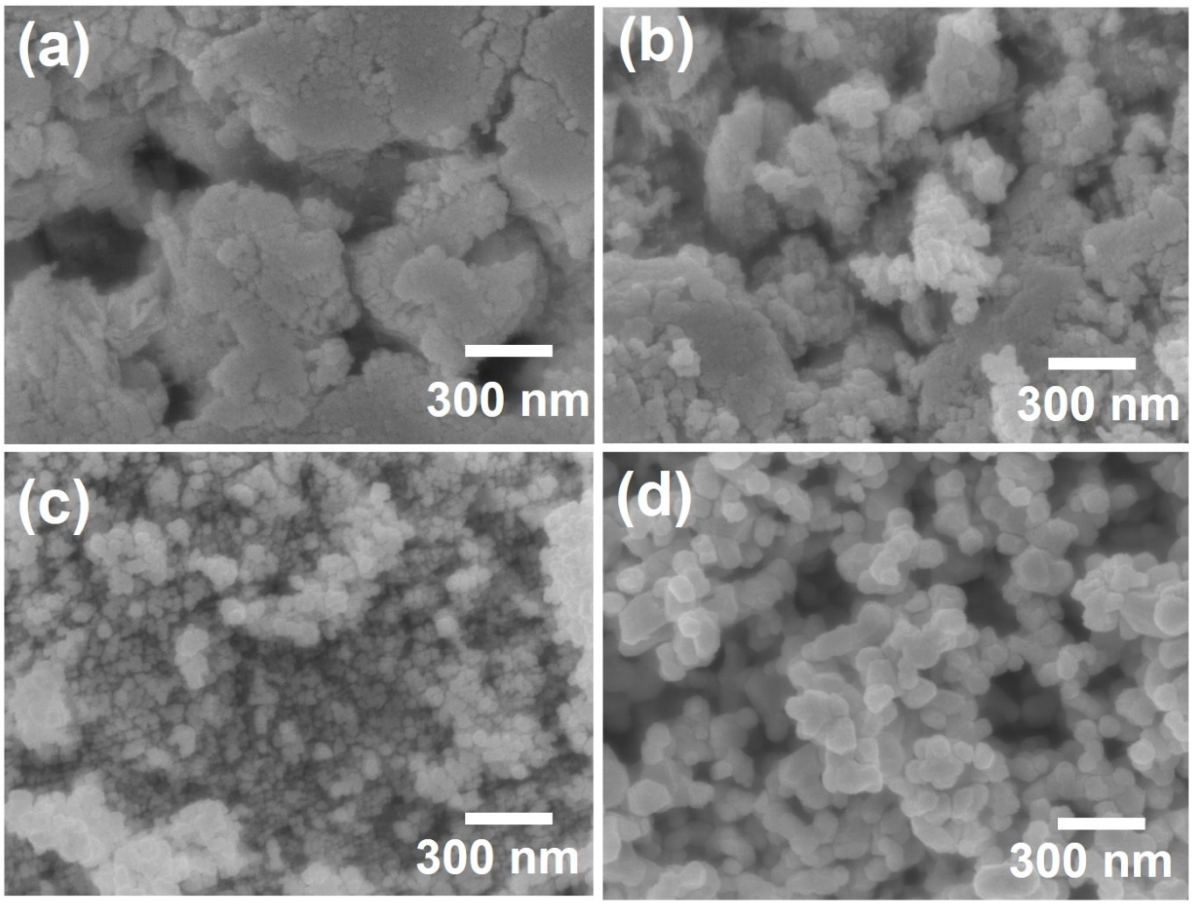

Figure S1. SEM images of (a) as-synthesized, and (b) 300 °C, (c) 600 °C, and (d) 900 °C heat treated samples.

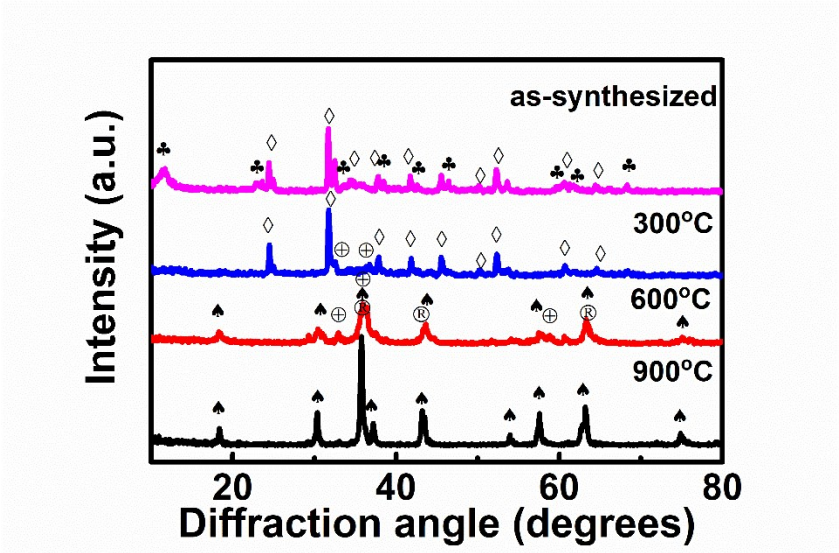

Figure S2. XRD patterns of as-synthesized and heat treated samples. '♣' represents hydroxylcarbonate compounds, '◊' represents carbonate compounds, '⊕' represents hexagonal structure (trivalent oxides), '®' represents rock-salt structure, and '♠' represents spinel structure.

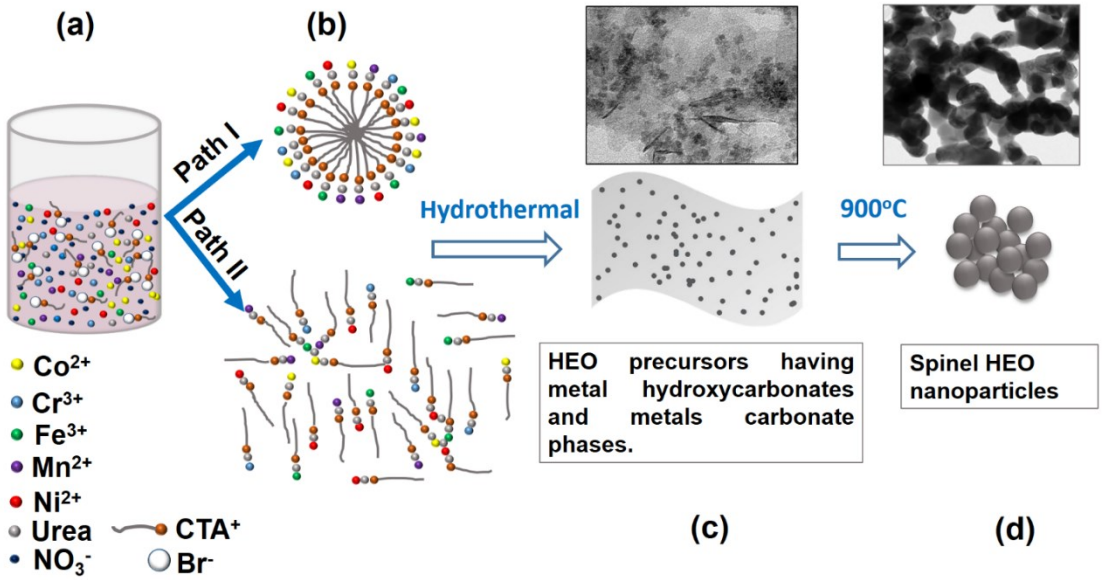

Figure S3. Formation mechanism of HESO NPs.

(a) Precursor solution consists of appropriate amounts of the nitrate salts in de-ionized water, CTAB, and urea.

(b) In the solution, there are two paths (Paths I and II) to form complex, in which metal ions are attached to CTAB. In Path I, the CTAB monomers form micelles and individual metal ions are attracted by micelles to become growth units. This type of units is stabilized, in part by the OH^- and CO_3^{2-} produced from the hydrolysis of urea (Reactions 1-3).[1] In Path II, metal ion clusters, with enclosing OH^- and CO_3^{2-} to hold the ions, are captured and shared by several CTAB monomers from different CTAB branches to form different units.

(c) Subsequently, hydroxycarbonate and carbonate compounds form during the hydrothermal treatment due to the reactions among the metal ions, OH^-, and CO_3^{2-} (Reactions 4 and 5).[1] The compounds exhibit nanoparticle and nanosheet morphologies due to the growth of Paths I and II, respectively.

(d) Finally, after the heat treatment at 900 °C, single-phase HESO nanoparticles (Reaction 6) are obtained.

$$CO(NH_2)_2 + H_2O \rightarrow 2NH_3 + CO_2 \quad (1)$$

$$CO_2 + H_2O \rightarrow CO_3^{2-} + 2H^+ \quad (2)$$

$$NH_3 + H_2O \rightarrow NH_4^+ + OH^- \quad (3)$$

$$M^{x+} + yCO_3^{2-} + xOH^- \rightarrow M(OH)_x{\cdot}(CO_3)_y \quad (4)$$

$$M^{2+} + CO_3^{2-} \rightarrow M(CO_3) \quad (5)$$

$$M(OH)_x(CO_3)_y;\ M(CO_3) \xrightarrow{\Delta} M_3O_4 + H_2O + CO_2 \quad (6)$$

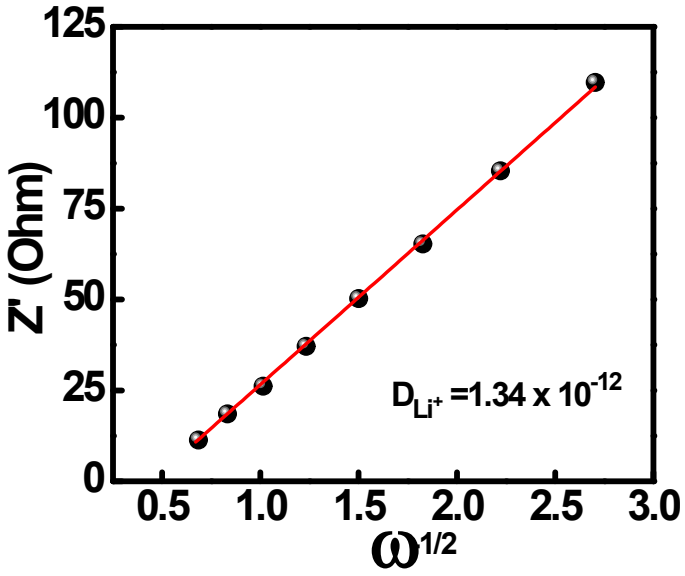

Figure S4. Plot of real part of impedance (Z′) in Warburg region as a function of inverse square root of angular frequency ($\omega^{-1/2}$) for HESO electrode.

Spinel oxide materials	Li^+ diffusion coefficient ($cm^2\ s^{-1}$)	Reference
Co_3O_4-graphene nanoflower	1.7×10^{-14}	[2]
$CoFe_2O_4$	1.1×10^{-13}	[3]
Fe_3O_4@rGO	9.3×10^{-13}	[4]
$MnCo_2O_4$	1.0×10^{-14}	[5]
$ZnMn_2O_4$	1.7×10^{-14}	[6]
$ZnCo_2O_4$@NiO/NF	1.8×10^{-14}	[7]
$(Mg_{0.2}Ti_{0.2}Zn_{0.2}Cu_{0.2}Fe_{0.2})_3O_4$	4.7×10^{-15}	[8]
This work	1.3×10^{-12}	-

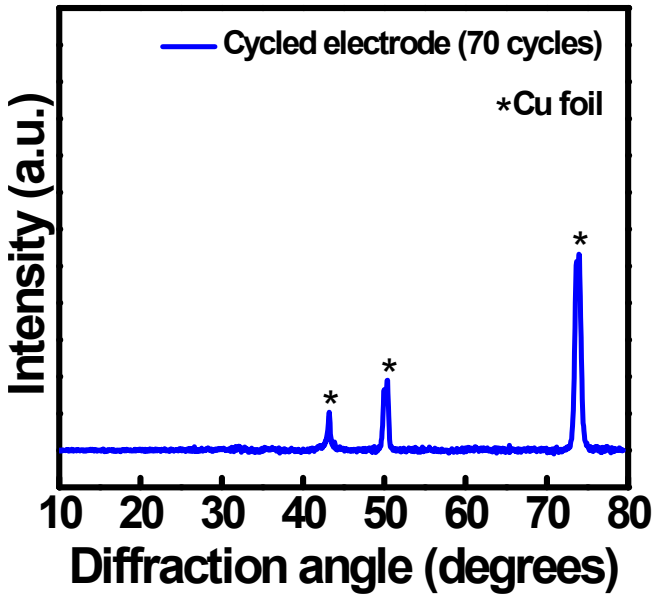

Figure S5. XRD pattern of HESO electrode after 70 charge-discharge cycles.

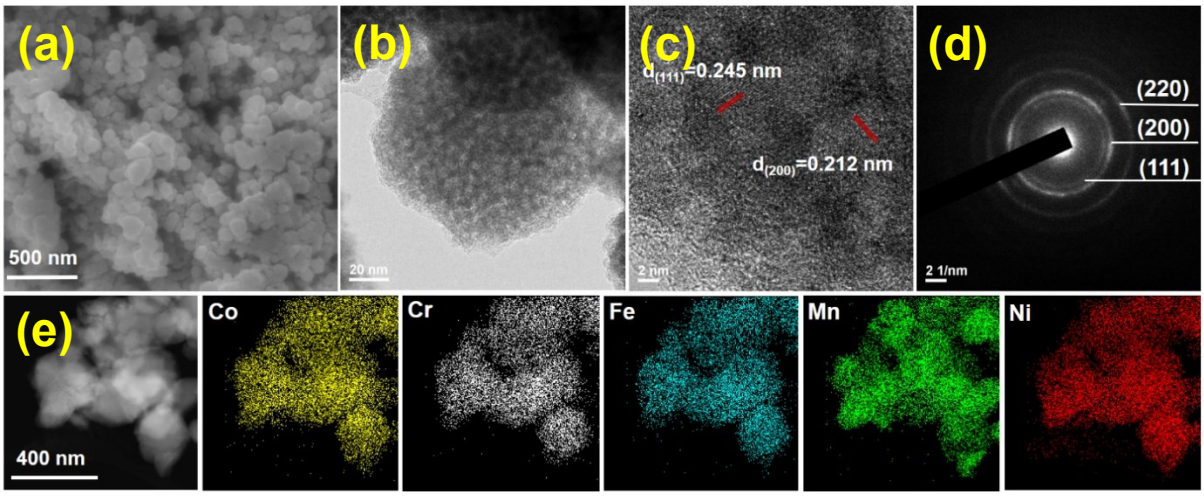

Figure S6. (a) SEM, (b) TEM, (c) HRTEM, (d) SAED, and (e) STEM mapping data of HESO NPs after70 charge-discharge cycles.

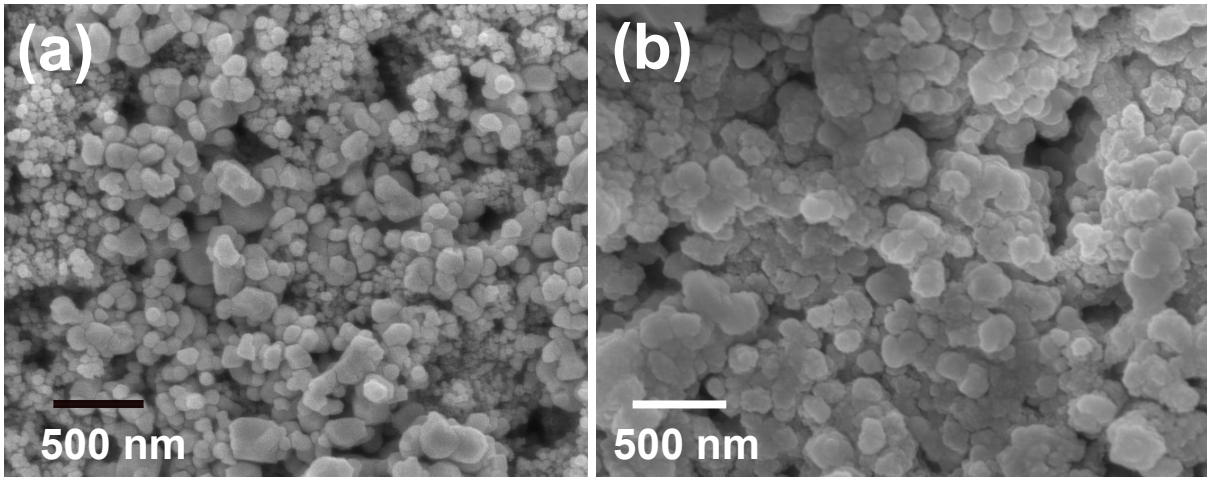

Figure S7. SEM images of HESO electrode (a) before and (b) after 200 charge-discharge cycles.

Reference

[1] S. Abouali, M. A. Garakani, Z.-L. Xu, J.-K. Kim, *Carbon* **2016**, *102*, 262-272.

[2] Y. Jiang, X. Yan, W. Xiao, M. Tian, L. Gao, D. Qu, H. Tang, *J. Alloys Compd.* **2017**, *710*, 114-120.

[3] Y.-Q. Chu, Z.-W. Fu, Q.-Z. Qin, *Electrochim. Acta* **2004**, *49*, 4915-4921.

[4] Y. Jiang, Z.-J. Jiang, L. Yang, S. Cheng, M. Liu, *J. Mater. Chem. A* **2015**, *3*, 11847-11856.

[5] G. Li, L. Xu, Y. Zhai, Y. Hou, *J. Mater. Chem. A* **2015**, *3*, 14298-14306.

[6] J. Zeng, Y. Ren, S. Wang, Y. Hao, H. Wu, S. Zhang, Y. Xing, *Inorganic Chemistry Frontiers* **2017**, *4*, 1730-1736.

[7] L. Zhang, S. Zhu, X. Li, H. Fang, L. Wang, Y. Song, X. Jia, *Ionics* **2019**, 1-8.

[8] H. Chen, N. Qiu, B. Wu, Z. Yang, S. Sun, Y. Wang, *RSC Adv.* **2020**, *10*, 9736-9744.